JOURNAL OF SOLID STATE CHEMISTRY **128,** 181–184 (1997)
ARTICLE NO. SC967177

Square Planar to Rectangular Distortion in Transition-Metal Compounds of Edge-Sharing Square Planar Units MX_4

N. Gupta, D.-K. Seo, and M.-H. Whangbo[1]

Department of Chemistry, North Carolina State University, Raleigh, North Carolina 27695-8204

and

S. Jobic, J. Rouxel, and R. Brec[1]

Laboratoire de Chimie des Solides, Institut des Materiaux de Nantes, UMR CNRS No. 110, Université de Nantes, 44072 Nantes Cedex 03, France

Received July 1, 1996; in revised form September 26, 1996; accepted October 1, 1996

In transition metal compounds of edge-sharing square planar MX_4 units (M = group 10, group 11; X = O, S, Se), a square planar to rectangular distortion is observed. The causes for this distortion in MX_2 ladder chains, M_3X_4 honeycomb layers, and 3D MX lattices were examined by performing extended Hückel tight binding electronic band structure calculations. The primary cause for the distortion is the reduction of the four-electron two-orbital destabilizing interactions among the p-orbitals of X.
© 1997 Academic Press

A number of transition-metal oxides and chalcogenides have structures based on edge-sharing square planar units MX_4 (X = O, S, Se). These structures range from one-dimensional (1D) "ladder" chains of formula MX_2 to two-dimensional (2D) "honeycomb" layers of formula M_3X_4 to three-dimensional (3D) lattices of formula MX. The MX_2 ladder chains (Fig. 1a) result from sharing the edges of square planar MX_4 units and are found in chalcogenides A_2MX_2 (A = alkali metal, M = group 10 element, X = chalocogen) (1) and oxides $ACuO_2$ (A = alkali metal) (2–4). For convenience of discussion, the shared X–X edge of an MX_4 unit will be referred to as X–$X(\perp)$, and the unshared X–X edge as X–$X(\parallel)$. In M_3X_4 honeycomb layers (Fig. 1b) of chalcogenides $A_2M_3X_4$ (5), every six MX_4 units form a hexagonal cylinder and every three MX_4 units share a common edge X–$X(\perp)$. The 3D MX lattices (Fig. 1c) of PdO (6), PtO (6) and PtS (7) can be constructed in terms of MX_2 ladder chains as follows: first, form layers of equally-spaced MX_2 chains with the spacing of X–$X(\parallel)$ and with the X–$X(\perp)$ edges perpendicular to the ab-plane, then stack these layers along the c-direction such that the chains of adjacent layers are perpendicular, and finally share the X atoms of adjacent layers so that the X–$X(\perp)$ edges form straight lines along the c-direction. The 3D MX lattices of CuO (8) and AgO (9) differ slightly from those of PdO, PtO, and PtS in that the MX_4 planes of the MX_2 chains are not perpendicular to the ab-plane (tilted by 11° from the perpendicular arrangement in CuO), and the MX_2 chains of adjacent layers are not orthogonal (twisted by 8° from the orthogonal arrangement in CuO).

All the 1D, 2D, and 3D compounds of edge-sharing MX_4 units mentioned above have a common structural feature that the MX_4 units are elongated along the edge-sharing directions so that X–$X(\parallel) > X$–$X(\perp)$. In their electronic structure study of the PtS_2^{2-} ladder chains of A_2PtS_2 (A = K, Rb) (1b), Silvestre and Hoffmann (10) noted that the elongation of the PtS_4 units is largely caused by the four-electron two-orbital destabilization (11) associated with the sulfur lone pairs. In the present work, we explore this point in more detail by studying the electronic band structures of representative MX_2 ladder chain, M_3X_4 honeycomb layer and 3D MX lattice systems using the extended Hückel tight binding (EHTB) method (12). The atomic parameters used in the present calculations are summarized in Table 1.

To describe the square planar to rectangular distortion of an MX_4 unit, we define the X–M–X angle such that X–$X(\parallel) > X$–$X(\perp)$ when the angle is smaller than 90° and also employ the coordinate systems shown in Fig. 1. Table 2 summarizes the X–M–X angles observed for representative 1D, 2D, and 3D compounds of edge-sharing square planar MX_4 units, e.g., the ladder chains of K_2PtS_2 (1b) and $NaCuO_2$ (3e), the honeycomb layers of $Cs_2Pt_3S_4$

[1] To whom correspondence should be addressed.

0022-4596/97 $25.00
Copyright © 1997 by Academic Press
All rights of reproduction in any form reserved.

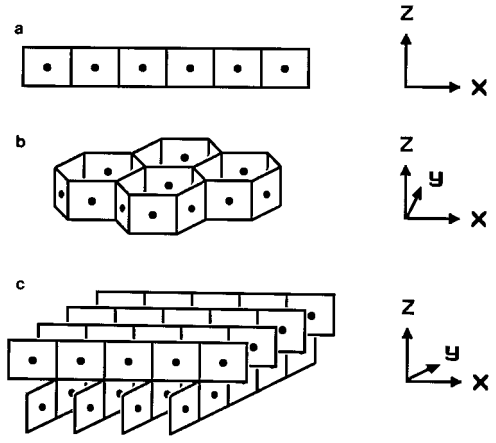

FIG. 1. Schematic perspective views of (a) an MX_2 ladder chain, (b) an M_3X_4 honeycomb layer, and (c) a 3D MX lattice.

TABLE 1
Exponents ζ_i and Valence Shell Ionization Potentials H_{ii} of Slater-Type Orbitals χ_i Used for EHTB Calculation[a]

Atom	χ_i	H_{ii} (eV)	ζ_i	c_i[b]	$\zeta_{i'}$	c_2[b]
O	2s	− 32.3	2.275			
O	2p	− 14.8	2.275			
S	3s	− 20.0	1.817			
S	3p	− 13.3	1.817			
Cu	4s	− 11.4	2.20			
Cu	4p	− 6.06	2.20			
Cu	3d	− 14.0	5.95	0.5933	2.30	0.5744
Pt	6s	− 9.08	2.554			
Pt	6p	− 5.47	2.554			
Pt	5d	− 12.6	6.013	0.6334	2.696	0.5513

[a] H_{ii}'s are the diagonal matrix elements $\langle\chi_i|H^{\text{eff}}|\chi_i\rangle$, where H^{eff} is the effective Hamiltonian. In our calculations of the off-diagonal matrix elements $H^{\text{eff}} = \langle\chi_i|H^{\text{eff}}|\chi_j\rangle$, the weighted formula was used (Ammeter et al., *J. Am. Chem. Soc.* **100,** 3686 (1978)).
[b] Contraction coefficients used in the double-ζ Slater-type orbital.

(5d) and the 3D lattice of PtO (6). The optimum X–M–X angles of these systems were calculated using the EHTB method while keeping the M–X bond lengths constant. As summarized in Table 2, the optimum X–M–X angles are all calculated to be smaller than 90° in good agreement with experiment.

For the square planar to rectangular distortion, the important orbitals to consider are the ones that lead to the top of the p-block bands. Such orbitals are given by the most antibonding combinations of the p-orbitals of X and are not stabilized by any d orbital of M due to a symmetry mismatch. For an MX_2 ladder chain, the p_x orbital of each X atom leads to the most sigma antibonding level **1**.

1

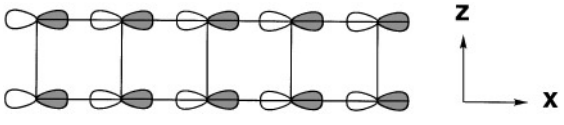

This level can be stabilized by the upper p_x orbital of M (e.g., $6p_x$ of Pt), but this is not effective. The antibonding in **1** is most effectively reduced by lengthening the X–$X(\|)$ distance, i.e., by decreasing the X–M–X angle from 90°. The most sigma antibonding level resulting from the p_z orbital of each X atom is **2**.

2

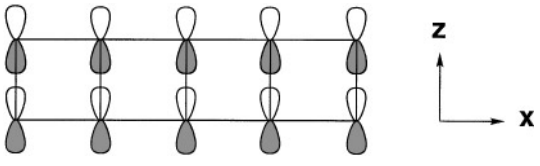

The extent of the antibonding in **2** is enhanced by decreasing the X–M–X angle from 90° because it shortens the X–$X(\perp)$ distance. In the level **2**, sigma antibonding is present in every isolated "X–$X(\perp)$ dimer" unit. If one views the level **1** in terms of "X–$X(\|)$ dimer" units, then the level **1** results when their sigma antibonding levels are combined in a σ antibonding manner between every adjacent dimer units.

TABLE 2
Experimental and Calculated X–M–X angles for the MX_4 Units in the Ladder Chains of K_2PtS_2 and $NaCuO_4$, the Honeycomb Layers of $Cs_2Pt_3S_4$, and the 3D Lattice of PtO

		Chain		Layer	3D Lattice
Parameter		K_2PtS_2	$NaCuO_2$	$Cs_2Pt_3S_4$	PtO
M–X–M (°)	Exptl.	80.8	33.6	81.4[b]	82.6
	Calc.	84	81	78	84
M–X (Å)[a]		2.358	1.840	2.407[b]	2.023

[a] The M–X bond lengths of the MX_4 units used for calculations.
[b] The $Pt_3S_4^{2-}$ honeycomb layer consists of two slightly different PtS_4 rectangles, and hence there are two different S–Pt–S angles (82.7° and 80.1°) and two different Pt–S bond lengths (2.428 and 2.387 Å). The values listed are the average values, and all PtS_4 units were assumed to be identical for calculations.

Therefore, the level **1** is more antibonding than is the level **2**, so that the square planar to rectangular distortion proceeds by increasing the X–$X(\|)$ distance. This trend can be seen from the projected density of state (PDOS) plots of the PtS_2^{2-} ladder chain calculated for the S–Pt–S angles of 80° and 100° (Fig. 2).

In an M_3X_4 honeycomb layer, each atom X has two p orbitals (i.e., p_x and p_y orbitals contained in the ab-plane of the layer) to make extensive σ antibonding interactions as in the orbital **1** for an MX_2 ladder chain. The PDOS plots of the $Pt_3S_4^{2-}$ layer calculated for the S–Pt–S angles of 80° and 100° (Fig. 3) show that the reduction of the antibonding associated with these p orbitals is important for the distortion decreasing the S–Pt–S angle from 90°. In a 3D MX lattice, each p orbital of X can make extensive σ antibonding interactions. Nevertheless, the square planar to rectangular distortion takes place to decrease the X–M–X angle from 90°. It is understandable because this distortion lowers the extensive antibonding interactions associated with *two* p orbitals (i.e., p_x and p_y) of each X, as illustrated by the PDOS plots of PtO calculated for the O–Pt–O angles of 80° and 100° (Fig. 4).

As already mentioned, in the 3D MX lattices of CuO and AgO, the MX_4 planes of the MX_2 chains are not perpendicular to the ab-plane, and the MX_2 chains of adjacent layers are not orthogonal. CuO and AgO contain one more valence electron per unit cell than do PdO, PtO, and PtS, so that the highest filled level of a local MX_4 unit in CuO and AgO is given by the orbital **3**.

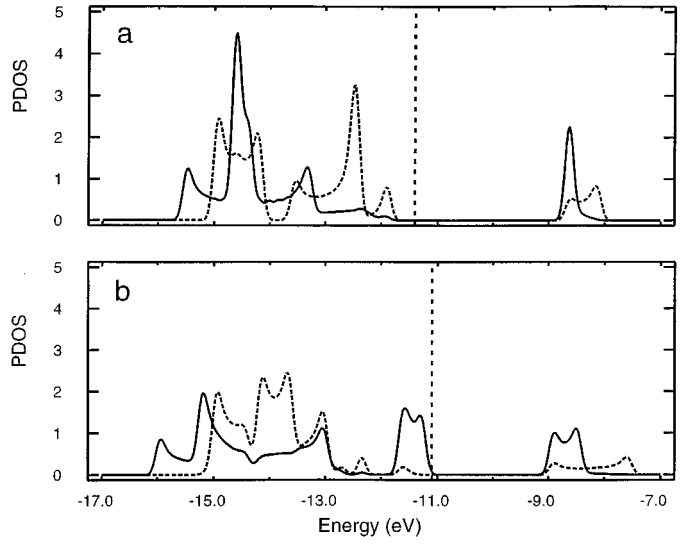

FIG. 2. PDOS plots of the PtS_2^{2-} ladder chain calculated for the S–Pt–S angles of (a) 80° and (b) 100°. The solid line represents the contribution of the sulfur p_x orbital, and the dotted line that of the sulfur p_z orbital. For simplicity, other orbital contributions are not shown. The vertical dashed line shows where the highest occupied level of the system lies.

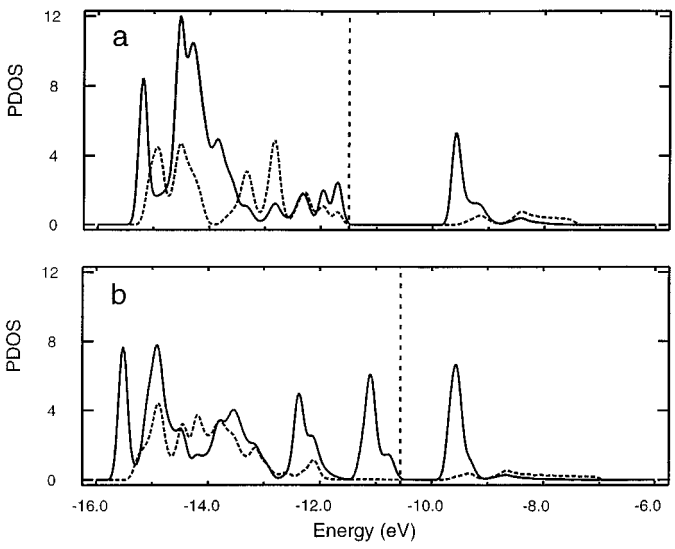

FIG. 3. PDOS plots of the $Pt_3S_4^{2-}$ honeycomb layer calculated for the S–Pt–S angles of (a) 80° and (b) 100°. The solid line represents the contribution of the sulfur p_x and p_y orbitals, and the dotted line that of the sulfur p_z orbital. For simplicity, other orbital contributions are not shown. The vertical dashed line shows where the highest occupied level of the system lies.

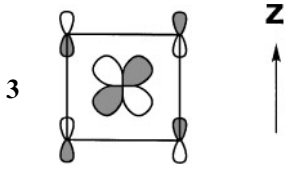

The latter has σ antibonding interactions involving p_z orbitals of X along X–$X(\perp)$, so its occupation enhances the antibonding associated with the p_z orbitals along the c-direction. The extent of this antibonding is reduced by decreasing the sigma overlap between adjacent p_z orbitals along the X–$X(\perp)$ direction. The tilting and twisting of the MX_2 chains found in CuO and AgO decrease the σ overlap, because they prevent the X–$X(\perp)$ linkages from forming a straight line along the c-direction.

In summary, EHTB calculations were carried out to probe the primary cause for square planar to rectangular distortions in compounds of edge-sharing square planar MX_4 units. In the A_2MX_2 and $ACuO_2$ chain and the $A_2M_3X_4$ honeycomb layer systems, the observed distortion is similar for different alkali metal atoms A so that the countercations have little effect on the observed distortion. For the MX_2 ladder chain, M_3X_4 honeycomb layer and 3D MX lattice systems, the overlap populations of the X–$X(\perp)$ and X–$X(\|)$ sides calculated in our work (not shown) are

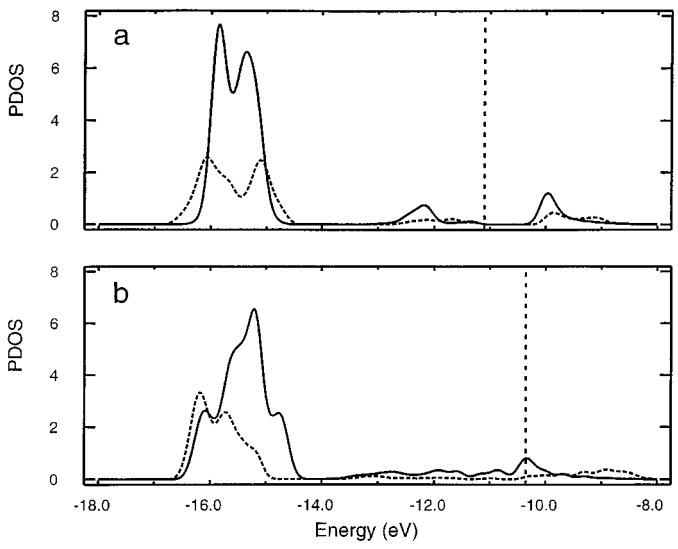

FIG. 4. PDOS plots of the PtO calculated for the O–Pt–O angles of (a) 80° and (b) 100°. The solid line represents the contribution of the oxygen p_x and p_y orbitals, and the dotted line that of the oxygen p_z orbital. For simplicity, other orbital contributions are not shown. The vertical dashed line shows where the highest occupied level of the system lies.

too small (in the third decimal place) for meaningful discussion. Our work indicates that as found for the case of the MX_2 ladder chains (10), the primary cause for the distortion in M_3X_4 honeycomb layers and 3D MX lattices is to reduce the extent of the four-electron two-orbital destabilizing interactions among the p orbitals of X.

ACKNOWLEDGMENTS

This work was supported by the Office of Basic Energy Sciences, Division of Materials Sciences, U.S. Department of Energy, under Grant DE-FG05-86ER45259, and by the European Community under the Human Capital and Mobility Project (ERBCHRXCT940675).

REFERENCES

1. (a) W. Bronger, S. Jäger, R. Rennau, and D. Schmitz, *J. Less-Common Met.* **154,** 261 (1989). (b) W. Bronger and O. Guenther, *J. Less-Common Met.* **27,** 73 (1972).
2. (a) R. Berger, and L.-F. Tergenius, *J. Alloys Comp.* **203,** 889 (1994). (b) W. Utsumi, K. Imai, M. Koike, H. Takei, T. Yagi, H. Takahashi, and N. Mori, *J. Solid State Chem.* **107,** 507 (1993). (c) K. Imai, M. Koike, H. Sawa, and H. Takei, *J. Cryst. Growth* **128,** 808 (1993). (d) K. Imai, M. Koike, H. Takei, H. Sawa, D. Shiomi, K. Nozawa, and M. Kinoshita, *J. Phys. Soc. Jpn.* **61,** 1819 (1992).
3. (a) T. Mizokawa, A. Fujimori, H. Namatame, K. Akeyama, and N. Kosugi, *Phys. Rev. B* **49,** 7193 (1994). (b) S. Nimkar, D. D. Sarma, and H. R. Krishnamurthy, *Phys. Rev. B* **47,** 10927 (1993). (c) T. Mizokawa, H. Namatame, A. Fujimori, K. Akeyama, H. Kondoh, H. Kuroda, and N. Kosugi, *Phys. Rev. Lett.* **67,** 1638 (1991). (d) K. Okada, A. Kotani, B. T. Thole, and C. A. Sawatzky, *Solid State Commun.* **77,** 835 (1991). (e) J. Pickardt, W. Paulus, M. Schmalz, and R. Schöllhorn, *J. Solid State Chem.* **89,** 308 (1990). (f) P. Steiner, V. Kinsinger, I. Sander, S. Hüfner C. Politis, R. Hoppe, and H. P. Müller, *Z. Phys. B* **67,** 497 (1987). (g) K. Hestermann, and R. Hoppe, *Z. Anorg. Allg. Chem.* **367,** 261 (1969).
4. (a) N. Brese, M. O'Keeffe, R. B. von Dreele, and V. G. Young, Jr., *J. Solid State Chem.* **83,** 1 (1989). (b) K. Hestermann and R. Hoppe, *Z. Anorg. Allg. Chem.* **367,** 249 (1969).
5. (a) S. H. Elder, S. Jobic, R. Brec, M. Gelabert, and F. J. DiSalvo, *J. Alloy Comp.* **235,** 135 (1996). (b) W. Bronger, R. Rennau, and Schmitz, *Z. Anorg. Allg. Chem.* **597,** 27 (1991). (c) J. Huster and W. Bronger, *J. Solid State Chem.* **11,** 254 (1974). (d) O. Günther and W. Bronger, *J. Less-Common Met.* **31,** 255 (1973).
6. W. J. Moore, Jr. and L. Pauling, *J. Am. Chem. Soc.* **63,** 1392 (1941).
7. A. Kjekshus, *Acta Chem. Scand.* **20,** 577 (1966).
8. S. Åsbrink and L.-J. Norrby, *Acta Crystallogr B* **26,** 8 (1970).
9. A. J. Salkind and W. C. Zeek, *J. Electrochem. Soc.* **106,** 366 (1959).
10. J. Silvestre and R. Hoffmann, *Inorg. Chem.* **24,** 4108 (1985).
11. T. A. Albright, J. K. Burdett, and M. H. Whangbo, "Orbital Interactions in Chemistry." Wiley, New York, 1985.
12. M.-H. Whangbo, and R. Hoffmann, *J. Am. Chem. Soc.* **100,** 6093 (1978).